

*Defect Measurements of CdZnTe Detectors Using  
I-DLTS, TCT, I-V, C-V and  $\gamma$ -ray Spectroscopy*

**R. Gul, Z. Li, R. Rodriguez, K. Keeter, A. Bolotnikov, and  
R. James**

*Presented at the 2008 SPIE Conference  
San Diego, CA  
August 11-14, 2008*

February 2009

**Nonproliferation and National Security Department**

**Brookhaven National Laboratory**

P.O. Box 5000  
Upton, NY 11973-5000  
[www.bnl.gov](http://www.bnl.gov)

Notice: This manuscript has been authored by employees of Brookhaven Science Associates, LLC under Contract No. DE-AC02-98CH10886 with the U.S. Department of Energy. The publisher by accepting the manuscript for publication acknowledges that the United States Government retains a non-exclusive, paid-up, irrevocable, world-wide license to publish or reproduce the published form of this manuscript, or allow others to do so, for United States Government purposes.

This preprint is intended for publication in a journal or proceedings. Since changes may be made before publication, it may not be cited or reproduced without the author's permission.

## DISCLAIMER

This report was prepared as an account of work sponsored by an agency of the United States Government. Neither the United States Government nor any agency thereof, nor any of their employees, nor any of their contractors, subcontractors, or their employees, makes any warranty, express or implied, or assumes any legal liability or responsibility for the accuracy, completeness, or any third party's use or the results of such use of any information, apparatus, product, or process disclosed, or represents that its use would not infringe privately owned rights. Reference herein to any specific commercial product, process, or service by trade name, trademark, manufacturer, or otherwise, does not necessarily constitute or imply its endorsement, recommendation, or favoring by the United States Government or any agency thereof or its contractors or subcontractors. The views and opinions of authors expressed herein do not necessarily state or reflect those of the United States Government or any agency thereof.



# Defect Measurements in CdZnTe Detectors Using I-DLTS, TCT, I-V, C-V and $\gamma$ -ray Spectroscopy

R. Gul<sup>1,2</sup>, Z. Li<sup>1</sup>, R. Rodriguez<sup>2</sup>, K. Keeter<sup>2</sup>, A. Bolotnikov<sup>1</sup>, R. James<sup>1</sup>.

1. Brookhaven National Laboratory, Upton, NY 11973

2. Idaho State University, Pocatello, Idaho, 83209

## ABSTRACT

In this work we measured the crystal defect levels and tested the performance of CdZnTe detectors by diverse methodologies, viz., Current Deep Level Transient Spectroscopy (I-DLTS), Transient Current Technique (TCT), Current and Capacitance versus Voltage measurements (I-V and C-V), and gamma-ray spectroscopy. Two important characteristics of I-DLTS technique for advancing this research are (1) it is applicable for high-resistivity materials ( $>10^6 \Omega\text{-cm}$ ), and, (2) the minimum temperature for measurements can be as low as 10 K. Such low-temperature capability is excellent for obtaining measurements at shallow levels.

We acquired CdZnTe crystals grown by different techniques from two different vendors and characterized them for point defects and their response to photons. I-DLTS studies encompassed measuring the parameters of the defects, such as the energy levels in the band gap, the carrier capture cross-sections and their densities. The current induced by the laser-generated carriers and the charge collected (or number of electrons collected) were obtained using TCT that also provides the transport properties, such as the carrier life time and mobility of the detectors under study. The detector's electrical characteristics were explored, and its performance tested using I-V, C-V and gamma-ray spectroscopy.

**Keywords:** CdZnTe detectors, Crystal defects, DLTS, gamma-ray spectroscopy

## 1. INTRODUCTION

For the past two decades CdZnTe has been considered as an attractive and suitable candidate for room-temperature x-ray and gamma-ray detectors. Its high band gap, relatively high density and atomic weight, high resistivity entailing a low leakage current, and, perhaps most importantly, its electron drift length have brought it to the attention of researchers and entrepreneurs. CdZnTe detectors are known for their high radiation-detection efficiency, position sensitivity, high stopping power, good energy-resolution, low power-consumption, low electronic-noise and portability at room temperature. All these required characteristics for a reliable radiation detector make CdZnTe a good material for x-ray and gamma-ray-detectors in a variety of fields, such as medical imaging, space and astronomy, environmental- and national security- applications.

CdZnTe detectors were fabricated for the first time in 1990s, and subsequently, tremendous efforts [1] have been made to raise their efficiency and performance. They encompass improving techniques to grow CdZnTe crystals with minimal fabrication-related defects, increasing the effective radiation interaction area, optimizing the performance, characterization, and stability of devices, and attempting to make them more compact and durable.

In our research, we investigated the defects in two CdZnTe detector crystals from different manufacturers, eV Products and a local crystal grower at BNL, and explored their electrical- and radiation-response. The first sample, CZT 1-ev, from eV Products, was grown by the high-pressure Bridgman Technique [2-3]. The second crystal, CZT-21-2, was fabricated by the Floating Method at BNL (Gu et al [4]). This study is focused on measuring point-defect parameters, such as energy levels,  $E$ , in the band gap, carrier capture cross-sections  $\sigma$ , and defect densities  $N$ , within the band gap using the I-DLTS technique[5,6]. Electron life time  $\tau_e$ , mobility  $\mu$ , space charge density  $N_{eff}$ , and induced current caused by the laser generated carriers and collected charge (or number of electrons collected) using TCT [7]. We investigated the detector's electrical characteristics and tested its detection performance tests by using I-V, C-V and  $\gamma$ -Ray Spectroscopy.

## 2. EXPERIMENTAL

The two samples we characterized for defect-related parameters were CZT-1-ev and CZT-21-2; the latter includes 12.5 ppm In as a dopant. The dimensions of the detectors are about  $10 \times 10 \times 2 \text{ cm}^3$  for CZT-1-ev, and  $8 \times 8 \times 2 \text{ cm}^3$  for CZT-21-2. Au contacts are placed on their back and front sides. A thin (10 nm), 2mm diameter electronically active window is cut into the middle on the front side to allow laser light to penetrate into the detector, which helps in generating the free carriers needed for the I-DLTS- and TCT- measurements.

The system we used to study the deep levels in the crystals is a current DLTS system, especially designed for high-resistivity materials, such as CdZnTe and heavily irradiated Si. These materials' very low capacitance along with their frequency dependence imposes limits on using other techniques, such as capacitance DLTS. The main components of BNL's I-DLTS system are the following: 1) A cryogenic cooling system, consisting of a He cryostat (8-350K) with temperature controller SI9650; 2) an illumination system for defect filling, consisting of a laser- pulse generator HP 8110A that drives lasers with various wavelengths (660 nm to 1030 nm); 3) a Keithley 487 power supply to provide bias on samples; 4) a Keithley 428 current amplifier to amplify the current transient signal obtained from the charges emitted from filled defect levels; and, 5) a Tek-7704A oscilloscope to record the current transients. For our study on the CZT samples, the electron filling of the defect levels is done with by a 822nm IR laser, which has an absorption length in CZT equaling the sample's thickness ( $\sim 1 \text{ mm}$ ). We observed that this wavelength, with 10V bias and 4.5 m W power, maximizes the number of electrons generated (for filling defect levels) in the I-DLTS measurements. All systems were controlled by a PC running the LabView program and analyzed using software.

The second main experiment we undertook employed TCT. The setup consists of a Keithley 237 power supply; a LeCroy 1GHz Oscilloscope; and an Agilent 81110A pulse generator. The illumination system contains a 660nm red laser, operated by the Agilent 81110A pulse generator at parameters of 10 V in biasing, 10 ms in period, and 5 ns in pulse width. This illumination system generates sufficient numbers of charge carriers at the exposed surface (through the thin metal window) of the detector.

## 3. RESULTS AND DISCUSSIONS

We measured the detector's electrical response in the dark as well as in white light. There is a remarkable shift between them in the leakage current and capacitance, indicating that samples' light-sensing response is good. Fig. 1a and 1b, respectively, show the I-V and C-V characteristic plots for sample CZT-1-ev. The leakage current in the light is 100 times more than that in dark, while the capacitance increases by almost a factor of two. The measured capacitance is about  $10^{-12} \text{ F}$ . The second sample, CZT-21-2 showed a similar type of behavior for I-V and C-V characteristics (Fig. 2a and 2b). Resistivity calculated from the I-V measurement for CZT-1-ev and CZT-21-2, respectively, is  $7.20 \times 10^{10} \Omega \text{ cm}$  and  $2.62 \times 10^{10} \Omega \text{ cm}$ . The depletion voltage was determined from TCT measurements that are depicted later in Figs. 4b and 5b. Sample CZT-1-ev is depleted at about 800 V, and sample CZT-21-2 at about 600 V.

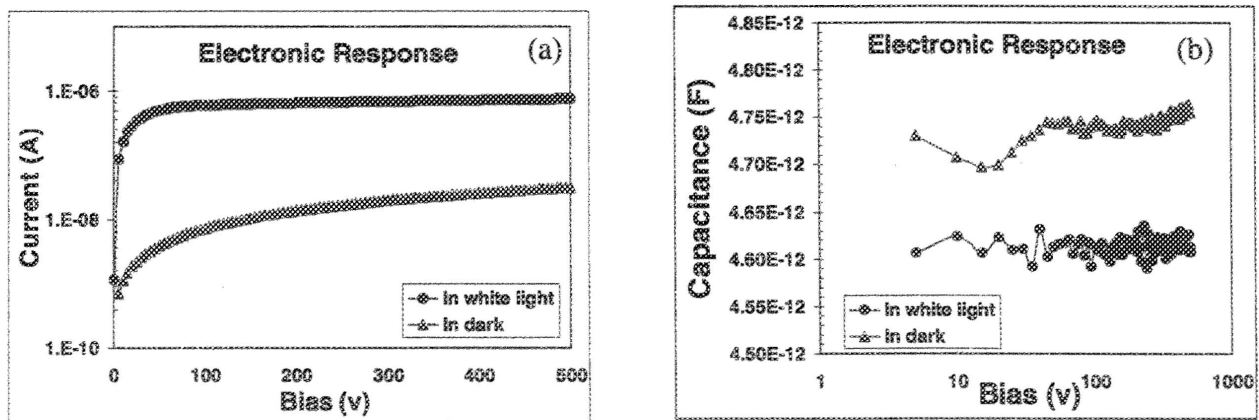


Fig. 1. Characteristic plots for the CZT-1-ev detector, a) Leakage current as a function of the applied bias voltage; b) Capacitance-voltage (C-V) plots in the dark and in white light.

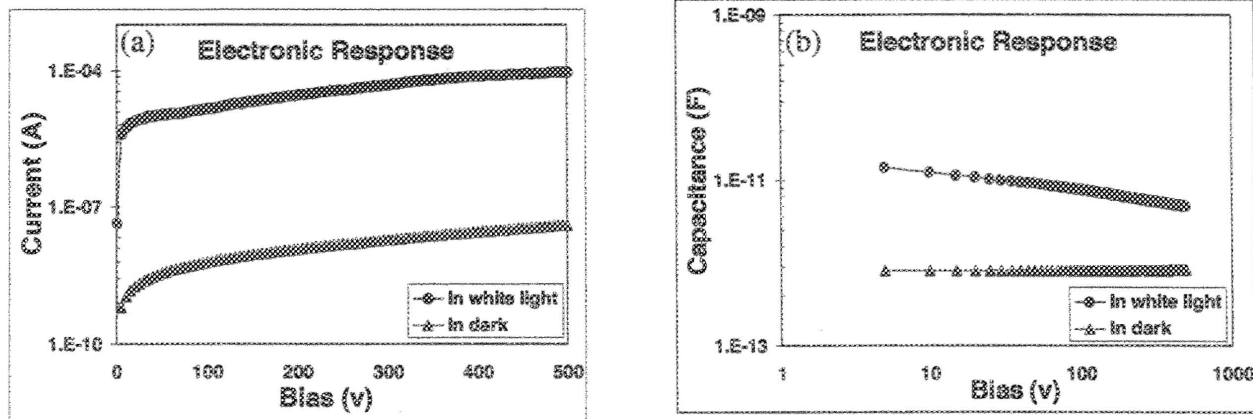


Fig. 2. Characteristic plots for the CZT-21-2 detector, a) Leakage current as a function of the applied bias voltage; b) Capacitance-voltage (C-V) plots in the dark and in white light.

The spectroscopic responses to gamma radiation of both samples were measured by using a standard  $\text{Am}^{241}$  source. Figs. 3a and 3b show the recorded spectra for the 59.6 keV photo peak.

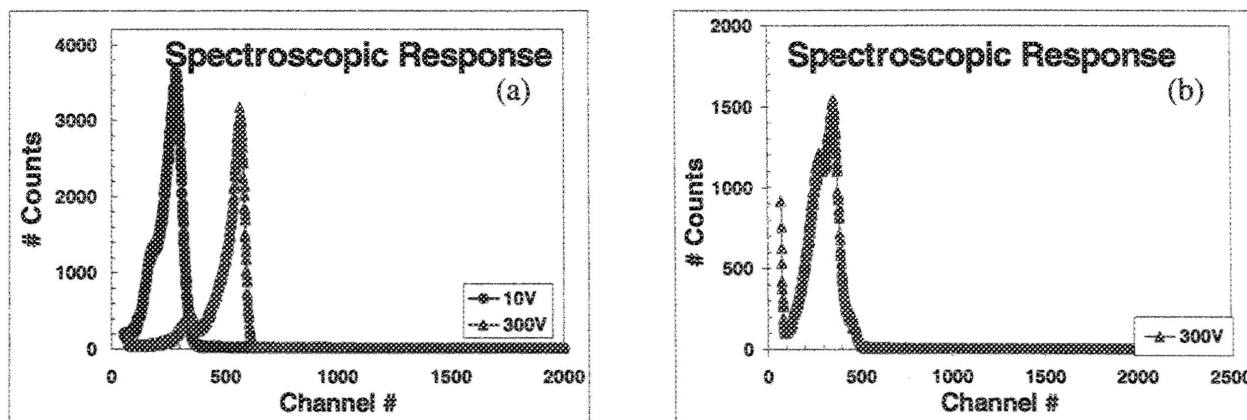
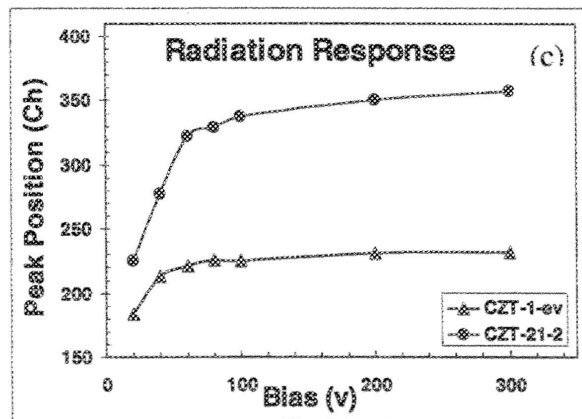


Fig 3. Energy spectrum measurements of 59.6 keV photo peak of  $\text{Am}^{241}$  by a) CZT-1-ev detector at 10 V and 300 V bias; b) CZT21-2 detector at 300 V bias; and, c) Detection of photo peak (position) as a function of bias voltage for the two detectors.

Figures 3a and 3b show the shift in the position of the photo peak with increasing bias, i.e., is the normal behavior of the detectors. The detector's photo detection response at various applied voltages across the devices is plotted in Fig. 3c. The  $\mu\tau_e$  for the first sample, CZT-1-ev, calculated from the  $\text{Am}^{241}$  gamma ray spectroscopy is  $4.9 \times 10^{-3} \text{ cm}^2/\text{V}$ . The manufacturer's value is  $7.8 \times 10^{-3} \text{ cm}^2/\text{V}$ . The  $\mu\tau_e$  for CZT-21-2 also determined from gamma ray spectroscopy is  $1.1 \times 10^{-3} \text{ cm}^2/\text{V}$ , while that quoted by the manufacturer is  $1.5 \times 10^{-3} \text{ cm}^2/\text{V}$ . The  $\mu\tau_e$  product is determined from classical Hecht equation below;



$$\eta(V) = \frac{V\mu\tau}{L^2} \left( 1 - \exp\left(-\frac{L^2}{V\mu\tau}\right) \right) \quad (1)$$

Here,  $\eta(V)$  is charge collection efficiency,  $V$  is the applied bias voltage, and  $L$  is the detector's thickness.

### 3.1. TCT results

We collected the data by applying voltage, starting at 100 V and going up to 1100 V. This range of applied voltage is comparatively four times higher than that for Si detectors. We recorded with an oscilloscope the current signal induced by the drift of the electron sheet, generated within one micron of the detector's surface, by the red laser illumination on the surface of the detector. Fig.4a illustrates the shape of the electron transient current at an applied bias of 1100 V for CZT-1-ev; the current falls with time, indicating a decreasing electric field from the front to the back side of the detector, or a positive space charge [8]. The second sample, CZT-21-2, exhibited similar behavior(Fig. 5a), although there is flat region near the end of the transient, indicating a space-charge region of much lower concentration near the back side than that near the front side. The maximum number of electrons collected are  $4 \times 10^8$  and  $2 \times 10^9$ , respectively, at 850 V and 600 V, while the maximum charge collected is, respectively,  $7 \times 10^{-11}$  C and  $3 \times 10^{-10}$  C (Figs. 4b and 5b). Correspondingly, the average number of electrons in the saturation region is  $4.14 \times 10^8$  and  $1.76 \times 10^9$ .

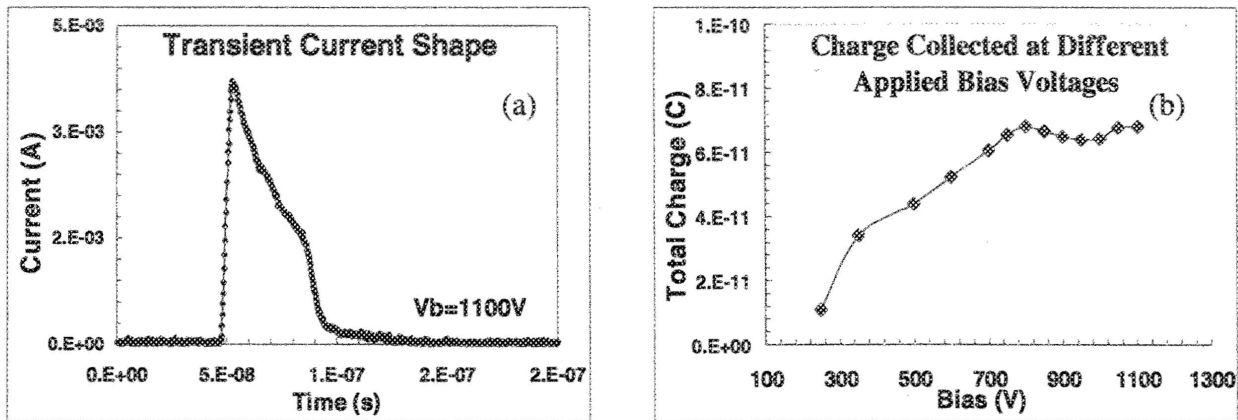


Fig. 4. TCT measurements for CZT-1-ev. a) Laser-induced transient current signal at 1100V bias voltage; b) Charge collection by the detector as a function of the applied voltage.

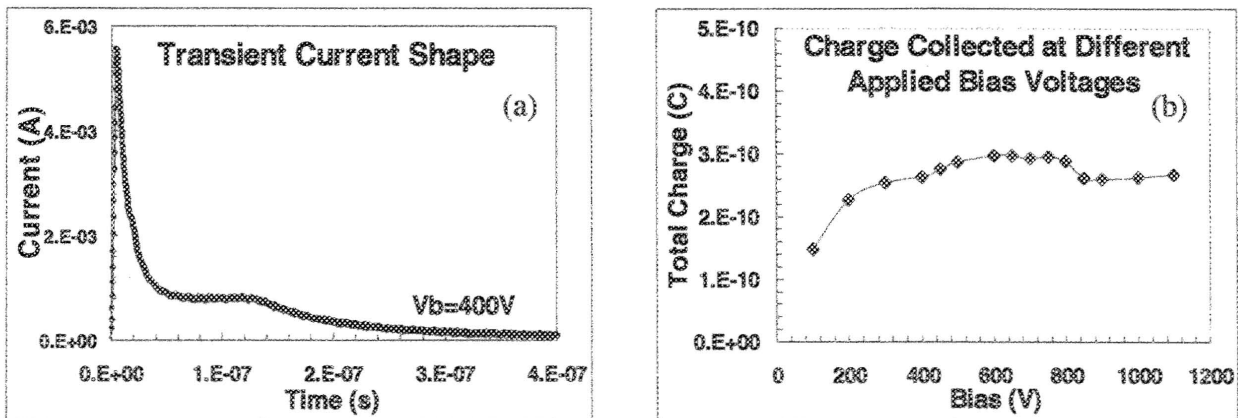


Fig. 5. TCT measurements for CZT-21-2. a) Laser-induced transient current signal at 1100V bias voltage; b) Charge collection by the detector as a function of the applied voltage.

We used the TCT data to determine the electric transport property,  $\mu$ , the electron mobility, and  $\tau_e$ , the electron life time. By measuring the transient time ( $t_{dr}$ ) of electrons (which is the width of the current transient pulse) at various bias voltages ( $V$ ) larger than the full depletion voltage, we can calculate electron mobility ( $\mu$ ) using the following expressions:

$$t_{dr} = \frac{d}{V_{dr}} = \frac{d}{\mu E} = \frac{d}{\mu \frac{V}{d}} = \frac{d^2}{\mu V} \quad (2)$$

Or

$$\frac{d^2}{t_{dr}} = \mu V, \quad (3)$$

where  $d$  is the detector's thickness. By plotting  $\frac{d^2}{t_{dr}}$  vs.  $V$ , as shown in Figs. 6a and 6b, we obtain the value of  $\mu$ , which is the slope of the plot.

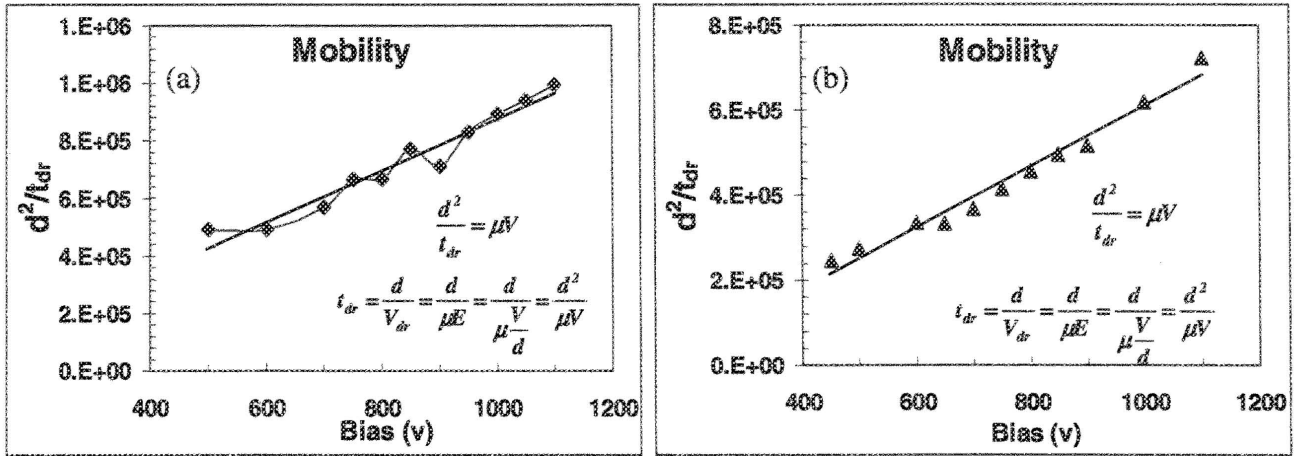


Fig. 6. Linear plots of  $d^2/t_{dr}$  as a function of the applied voltage to determine the mobility of electrons for a) CZT-1-ev; and, b) CZT-21-2.

The value for the  $\mu$  obtained from these plots is  $902 \text{ cm}^2/\text{sV}$  for CZT-1-ev and  $718 \text{ cm}^2/\text{s V}$  for CZT-21-2. Electron life time,  $\tau_e$ , calculated from the  $\mu\tau_e$  product measured previously is  $8.655 \times 10^{-6} \text{ s}$  for CZT-21-1, while for CZT-21-2 it is  $2.09 \times 10^{-6} \text{ s}$ . Table 1 summarizes the parameters determined from these data.

Table 1. Data obtained from I-V, C-V and TCT experiments. The collected charge for CZT-1-ev and CZT-21-2 were recorded at 1100V and 400V, respectively

Sample	$\rho$ ( $10^{10}$ $\Omega\text{cm}$ )	$\mu\tau$ ( $\text{cm}^2/\text{V}$ )	$\tau$ ( $\mu\text{s}$ )	$\mu$ $\text{cm}^2/\text{sV}$	Average # of $e^-$ Collected	Collected Charge (C)
CZT-1-ev	7.20	$3.9 \times 10^{-3}$	4.33	902	$4.14 \times 10^8$	$6.82 \times 10^{-11}$
CZT-21-2	2.62	$1.1 \times 10^{-3}$	1.53	718	$1.76 \times 10^9$	$2.62 \times 10^{-10}$

### 3.2. I-DLTS results

To obtain knowledge about the point defects through I-DLTS data, we first cooled the detector to about 10 K, and then heated it up at a constant rate to about 350 K. The ramp-up temperature step was about 1-1.2 K. At each temperature, the defect levels in a sample were first filled at 0 bias voltage and irradiated for 2 ms (pulse width) with an IR laser of 822 nm with a period of 45 ms and biased at 10 V laser bias. Then, during the time when the laser is on for a laser pulsing cycle (45 ms - 2 ms= 43 ms), a bias voltage was applied to the sample to efficiently de-trapping the charges from previously filled defect levels. The resulting transient current was recorded by the oscilloscope and the PC. We obtained the I-DLTS signal by sampling the difference in the current transient at two sampling times:  $t_1$  and  $t_2$  at each temperature. The sampling time  $t_1$  was increased in steps from 0.2 ms to 3 ms, while the sampling time  $t_2$  was taken as  $4t_1$ . Li gives more details of I-DLTS principles and modeling<sup>5</sup>. The energy levels, calculated from the transient I-DLTS signal, are electron traps and their energies are measured from the edge of the crystal's conduction band.

Fig.7a. plots the I-DLTS spectra for CZT-i-ev. There are three main peaks. Most traps are in the upper quarter of the band gap. We note the two prominent peaks connected to each other in the temperature range from 120 K to 220 K. The Arrhenius plots of  $t_1 T_{peak}^2$  Vs.  $1000/T_{peak}$  are shown in Fig. 7b, from which we obtain the energy level and cross section of the defect levels.

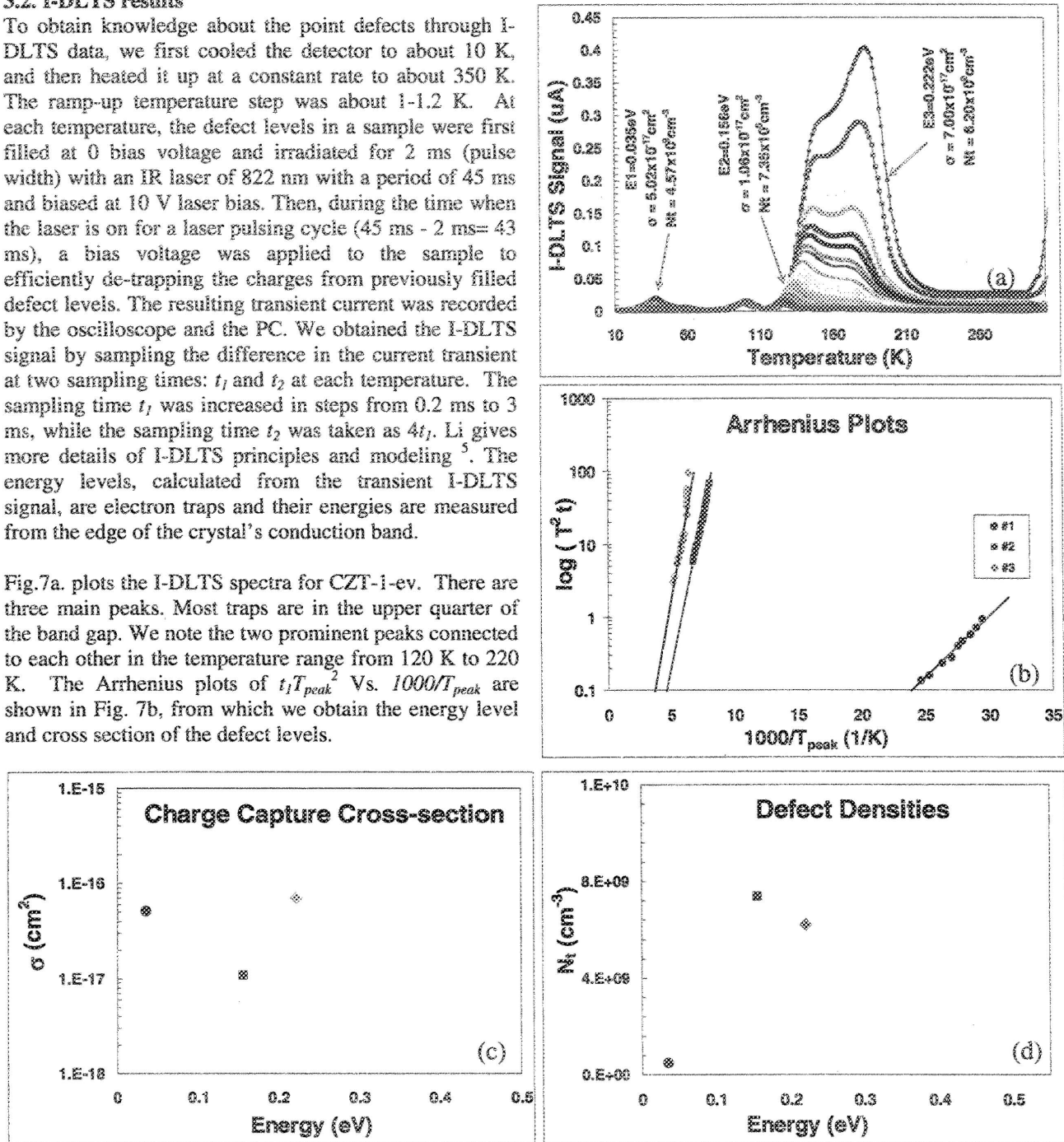


Fig.7. Defect information for CZT-i-ev by using I-DLTS; a) Identification of defect levels using different time windows. The plot also records the energy levels, carrier capture cross-sections, and the corresponding defect densities; b) Arrhenius plots; c) Charge capture cross-sections as a function of energy; and, d) Defect densities as a function of energy.

The first shallow level, observed in most CZT detectors, is 35 meV with a  $\sigma$  of  $5.02 \times 10^{-17} \text{ cm}^2$  and very low trap density of  $4.57 \times 10^8 \text{ cm}^{-3}$ . In the middle region of temperature, there are two very distinctive main deep levels of 156 meV and 222 meV with  $\sigma$  of  $1.06 \times 10^{-17} \text{ cm}^2$  and  $7.00 \times 10^{-17} \text{ cm}^2$  respectively. The trap densities are in the same range, viz.,  $7.35 \times 10^9 \text{ cm}^{-3}$  and  $6.20 \times 10^9 \text{ cm}^{-3}$ , respectively. The  $\sigma$  for the three traps is around  $10^{-17} \text{ cm}^2$ . Figs 7 c and 7d plot the

Table.2. Summary of the findings from I DLTS experiments

Sample	Trap #	E (meV)	$\sigma$ (cm <sup>2</sup> )	$N_t$ (cm <sup>-3</sup> )
CZT-1-ev	1	35	$5.02 \times 10^{-17}$	$4.57 \times 10^8$
	2	156	$1.06 \times 10^{-17}$	$7.35 \times 10^9$
	3	222	$7.00 \times 10^{-17}$	$6.20 \times 10^9$
CZT-21-2	1	11	$1.82 \times 10^{-19}$	$1.36 \times 10^{11}$
	2	14	$2.90 \times 10^{-20}$	$9.51 \times 10^{10}$
	3	173	$2.79 \times 10^{-14}$	$6.88 \times 10^{10}$
	4	244	$4.29 \times 10^{-15}$	$3.34 \times 10^{10}$
	5	270	$1.22 \times 10^{-18}$	$1.07 \times 10^{11}$
	6	456	$7.46 \times 10^{-16}$	$8.82 \times 10^{10}$

#### 4. CONCLUSIONS

I We investigated two detectors fabricated by two different techniques, i.e., the high-pressure Bridgman Technique, and the Floating Method. Both detectors have different numbers and types of electron trap levels in their crystal. Our comparison of their I-DLTS results suggests that the defect levels for the eV Product detector are half those of the other crystal grown at BNL. There are shallow- and middle-level traps in the crystal of the second detector. In the CZT-1-ev1 detector, the defect levels mostly are shallow electron traps, while, for the second detector, in addition to shallow-level traps, there are deep electron traps close to the mid band gap.

The electrical- and spectroscopic-responses of the detectors are quite different. There are clear correlations between the defect density and detector properties: the sample with fewer defects (CZT-1-ev) has an electron lifetime four times larger than the BNL one (CZT-21-2). The parameters of the point defects and the response of each detector to light, bias, and gamma radiations are related to the fabrication technique and growth environment of the crystals.

#### REFERENCES

- [1] Parnham, K.B., *Nucl. Instr. and Meth. A* 377, 487-491 (1996).
- [2] Kimura, H., Komiya, H., *J. Cryst. Growth* 20, 283-291 (1973).
- [3] Doty, F.P. et al., *J. Vac. Sci. Technol. B* 10 (4), 1418-1422 (1992).
- [4] Gu, G. D., *J. Cryst. Growth* 287, 318-322 (1993).
- [5] Li, Z., *Nucl. Instr. and Meth. A* 403, 399-416 (1998).
- [6] Li Z., Li, C.J., *Materials Science in Semiconductor Processing* 9, 283-287 (2006).
- [7] Eremin, V., *Nucl. Instr. and Meth. A* 372, 388-398 (1996).
- [8] Li, Z., *IEEE Trans. Nucl. Sci.*, vol. 51, 1901-1908 (2004).
- [9] Li, Z., *Nucl. Instr. and Meth. A* 377, 265-275 (1996).